jth

ORIGINAL ARTICLE

Soluble endoglin reduces thrombus formation and platelet aggregation via interaction with αIIbβ3 integrin

Elisa Rossi[1] | Miguel Pericacho[2] | Alexandre Kauskot[3] |
Luis Gamella-Pozuelo[2,4] | Etienne Reboul[1] | Alexandre Leuci[1] |
Cristina Egido-Turrion[2] | Divina El Hamaoui[1] | Aurore Marchelli[1] |
Francisco J. Fernández[4] | Isabelle Margaill[1] | M. Cristina Vega[4] |
Pascale Gaussem[1,5] | Samuela Pasquali[6] | David M. Smadja[1,5,7] |
Christilla Bachelot-Loza[1] | Carmelo Bernabeu[4]

[1]Innovative Therapies in Hemostasis, INSERM U1140, Université Paris Cité, Paris, France

[2]Department of Physiology and Pharmacology, Universidad de Salamanca, Salamanca, Spain

[3]HITh, INSERM UMR-S 1176, Université Paris-Saclay, Le Kremlin-Bicêtre, France

[4]Centro de Investigaciones Biológicas Margarita Salas, Consejo Superior de Investigaciones Científicas (CSIC), Madrid, Spain

[5]Service d'hématologie biologique, Hôpital Européen Georges Pompidou, AP-HP, Paris, France

[6]Cibles Thérapeutiques et Conception de Médicaments (CiTCoM), UMR8038 CNRS, Paris, France

[7]Laboratory of Biosurgical Research, Carpentier Foundation, Paris, France

Correspondence
Elisa Rossi, Faculty of Pharmacy, Hematology Department, Insert UMRS1140 – University of Paris, 4 Avenue de l'Observatoire, 75006 Paris, France.
Email: elisa.rossi@u-paris.fr

Present address
Francisco J. Fernández, Abvance Biotech srl, 32 Reina Victoria Av., 28003 Madrid, Spain.

Abstract

Background: The circulating form of human endoglin (sEng) is a cleavage product of membrane-bound endoglin present on endothelial cells. Because sEng encompasses an RGD motif involved in integrin binding, we hypothesized that sEng would be able to bind integrin αIIbβ3, thereby compromising platelet binding to fibrinogen and thrombus stability.

Methods: *In vitro* human platelet aggregation, thrombus retraction, and secretion-competition assays were performed in the presence of sEng. Surface plasmon resonance (SPR) binding and computational (docking) analyses were carried out to evaluate protein-protein interactions. A transgenic mouse overexpressing human sEng (*hsEng*[+]) was used to measure bleeding/rebleeding, prothrombin time (PT), blood stream, and embolus formation after FeCl$_3$-induced injury of the carotid artery.

Results: Under flow conditions, supplementation of human whole blood with sEng led to a smaller thrombus size. sEng inhibited platelet aggregation and thrombus retraction, interfering with fibrinogen binding, but did not affect platelet activation. SPR binding studies demonstrated that the specific interaction between αIIbβ3 and sEng and molecular modeling showed a good fitting between αIIbβ3 and sEng structures involving the endoglin RGD motif, suggesting the possible formation of a highly stable αIIbβ3/sEng. *hsEng*[+] mice showed increased bleeding time and number of rebleedings compared to wild-type mice. No differences in PT were denoted between genotypes. After FeCl$_3$ injury, the number of released emboli in *hsEng*[+] mice was higher and the occlusion was slower compared to controls.

Conclusions: Our results demonstrate that sEng interferes with thrombus formation

and stabilization, likely via its binding to platelet αIIbβ3, suggesting its involvement in primary hemostasis control.

KEYWORDS
endoglin, endothelial cells, integrins, platelet, thrombosis

1 | INTRODUCTION

Endoglin (Eng) is a membrane co-receptor for the transforming growth factor-beta (TGF-β) family that is overexpressed in proliferating endothelial cells and is involved in different cardiovascular conditions [1]. Mutations in the endoglin gene (ENG) cause hereditary hemorrhagic telangiectasia (HHT) type 1, a disease characterized by arteriovenous malformations in the brain, liver, and lung, as well as mucocutaneous telangiectases leading to epistaxis and gastrointestinal (GI) bleeding [2–4]. It is widely accepted that bleeding in HHT is mainly due to the rupture of the fragile nasal and GI telangiectases, but additional involvement of an abnormal hemostasis has been postulated in disease animal models of HHT [5,6]. In HHT1, haploinsufficiency of membrane-bound endothelial endoglin is at the molecular basis of blood vessel fragility and altered hemostasis [5,7]. In this line, we previously showed that the extracellular region of Eng has a role in hemostasis via the αIIbβ3 integrin-mediated adhesion of platelets to the endothelium and that its lack in mouse models of HHT ($Eng^{+/-}$) reduced platelets rolling on endothelium [5,6]. Thus, the interaction between endothelial Eng and platelet αIIbβ3 may contribute to platelet recruitment to the site of injury, a necessary step for the restoration of endothelial integrity [5,6].

In addition to the membrane form of Eng, a circulating soluble endoglin (sEng), released during proteolytic processing of membrane-bound Eng by the matrix metalloproteinase-14 (MMP14) or MMP12, was found [8–10]. Plasma levels of sEng in healthy individuals are around 2 to 6 ng/mL [11–13], but these values are upregulated in certain pathophysiological conditions. For example, sEng concentration increases in normotensive pregnant woman (7-20 ng/mL) and even further in women with preeclampsia (10-80 ng/mL) [12,14]. Of note, a correlation between increased circulating levels of sEng with the severity of preeclampsia and development of a rare life-threatening pregnancy complication of preeclampsia named hemolysis, elevated liver enzymes and low platelets (HELLP) has been reported [14,15–17]. Furthermore, the pathogenic role of sEng in preeclampsia-associated hypertension and renal involvement has been demonstrated in several *in vivo* studies [9,18–20]. Abnormal high levels of sEng are also found in other cardiovascular-related conditions such as atherosclerosis, hypercholesterolemia [21,22], diabetes mellitus [23–25], diabetic retinopathy [26], hypertension [23], circulatory failure in septic shock syndrome [27], coronary artery disease [28–30], acute myocardial

Essentials

- The circulating form of human endoglin (sEng) is a cleavage product of membrane-bound endoglin.
- sEng encompasses a sequence motif involved in binding to integrin αIIbβ3 from platelets.
- sEng reduces platelet aggregation and interferes with thrombus formation and stabilization.
- Eng is a new player in the control of primary hemostasis and thromboinflammatory processes.

infarction [31], and reperfusion after cerebral large-vessel occlusion [32]. These findings are in agreement with several *in vivo* and *in vitro* studies supporting an active role of sEng in endothelial dysfunction and vascular remodeling [33–35]. Increased circulating levels of sEng have also been proposed as a prognosis marker in cancer [36], including breast cancer [37], prostate cancer [38], colorectal cancer [39], or head and neck paragangliomas [40], and a marker of cancer metastasis [36,37,41]. In addition, patients receiving metastasis-positive chemotherapy with solid tumors showed markedly decreased sEng levels compared with those of a comparable untreated group of patients (median: 64.8 ng/mL vs 36.1 ng/mL, respectively), suggesting that sEng may be used for monitoring cancer relapse in a long-term follow-up [41]. At variance with the upregulated levels of sEng associated with the above-described pathological conditions, reduced shedding of sEng in patients with HHT1 has been reported; this is in agreement with the dominant transmission of this disease, leading to reduced expression of the endoglin protein [11,13].

Several lines of experimental evidence support a role for sEng in integrin-related activities. Thus, sEng has been shown to counteract the function of membrane-bound endoglin by competing with its binding to integrins such as α5β1 and αIIbβ3 [5,42,43]. Consequently, sEng can induce a vessel destabilization by interfering with the endothelial-perivascular cell interactions [43], as well as with the interactions between platelets and endothelial cells during rolling [5]. However, the role of sEng in hemostasis has not yet been thoroughly investigated. By using *in vitro* assays, computational analysis, and a transgenic mouse line overexpressing human sEng, we aimed to determine whether sEng would bind platelet αIIbβ3 to prevent

fibrinogen binding to platelets and how it could compromise the stability of the thrombus during clot formation.

2 | METHODS

2.1 | Human blood donors

Human blood from healthy donors was obtained from the French organization "Etablissement Français du Sang (EFS)" (convention C CPSL UNT N°12/EFS/064), and collected in either BD Vacutainer tubes containing ACD solution (5.7 mM citric acid, 11.2 mM trisodium citrate, and 20 mM dextrose; final concentrations) or tubes containing a solution of 3.2% sodium citrate.

2.2 | Soluble endoglin

Recombinant human endoglin/CD105 (sEng; R&D Systems, #1097-EN/CF; Supplementary Figure S1) was used for functional in vitro assays with platelets. For measuring protein-protein interactions by surface plasmon resonance, a streptavidin-tagged construct (sEng-Strep-tag II) of soluble endoglin [44] was used.

2.3 | In vitro thrombus formation under flow conditions

Aggregation under flow conditions was performed as previously described [45]. Briefly, total citrated blood was stained with 1 µg/mL calcein (Invitrogen), and this labeling was shown to neither induce nor alter platelet activation. A total of 10 different blood donors were used. Thrombus formation was evaluated in a whole blood perfusion assay on Cellix Vena8 chambers (V8CF-400-100-02P10, tebu-bio), previously coated homogeneously with a fibrillar collagen matrix (50 µg/mL, Stago) at 56 dynes/cm^2 to measure shear stress–linked to surface tension simulating arteriole flux [46] and then recorded for 5 minutes. Throughout the perfusion, the same field was observed to monitor platelet adhesion and aggregation. At the end of the infusion, 5 fields were analyzed and the averaged values for each donor (control [n = 5] vs 5 µg/mL of sEng [n = 5] and control [n = 5] vs 1 µg/mL of [sEng n = 5]) were calculated. Quantification was performed by measuring the calcein fluorescence defining the thrombus surface in µm^2. Thrombus formation was quantified (size cutoff = 10 µm^2, corresponding to, at least, 5 platelets) using Image J software, and the corresponding graph elaboration was performed by Graph-Pad Prism software.

2.4 | Washed platelet preparation

Whole blood collected on ACD tubes was centrifuged for 11 minutes at 216 g and 22 °C to obtain platelet-rich plasma (PRP). PRP was diluted with washing buffer (103 mM NaCl, 5 mM KCl, 2 mM CaCl$_2$, 1 mM MgCl$_2$, 5 mM glucose, and 36 mM citric acid; pH 6.5) containing the platelet inhibitor PGE1 (0.2 µM) and the ADP scavenger apyrase (1 U/mL; Sigma-Aldrich). The PRP suspension was centrifuged for 12 minutes at 1240× g and 22 °C to pellet the platelets. This washing step was repeated once with a washing buffer containing PGE1 and apyrase [47]. Platelets were finally resuspended at 3×10^8 platelets/mL in reacting buffer (10 mM HEPES, 140 mM NaCl, 3 mM KCl, 5 mM NaHCO$_3$, 5 mM MgCl$_2$, and 10 mM glucose; pH 7.35) in the presence of 2 mM CaCl$_2$. This reacting buffer was used as a negative control (vehicle) in sEng experiments.

2.5 | Platelet aggregation in microplates and aggregometry

Human washed platelets (3×10^8/mL) were preincubated in the presence of vehicle alone or sEng at 0.1, 1, or 5 µg/mL (R&D Systems, #1097-EN/CF) for 2 minutes at 37 °C under stirring in the wells of a 96-well microplate (half-area flat bottom; Greiner Bio-one). Then, aggregation was induced by adding 1 µM of TRAP6 (Bachem) or 0.5 µM of the thromboxane-prostanoid receptor agonist U46619 (Calbiochem, Merck). The extent of platelet aggregation was expressed as the percentage of maximal aggregation calculated as the change in absorbance at 405 nm relative to the absorbance under resting condition and after full platelet aggregation obtained with 10 µM thrombin receptor–activating peptide-6 (TRAP-6; Bachem), as previously described [45]. Platelet aggregation, performed under the same conditions as described above, was also measured using light transmission aggregometry (ChronoLog Aggregometer Model 700, Chronolog Corporation) [48] to confirm the microplate results.

2.6 | Clot retraction assay

Washed platelets were added in a tube of aggregometry (Bio/Data Corporation) at a final concentration of 2×10^8 platelets/mL in the presence of fibrinogen (0.5 mg/mL), as previously described [49]. The retraction was performed in the presence of various concentrations of sEng (0.1, 1, or 5 µg/mL) or vehicle upon preincubation at 37 °C for 5 minutes. Then, a solution of thrombin (Biopharm) and Ca^{2+} (2 IU/mL and 2 mM final concentrations, respectively) was added. The tubes were incubated at 37 °C for 30 minutes, and photographed every 5 minutes for clot sizing. The 2D size of the retracted clots was quantified with the NIH ImageJ software (http://rsb.info.nih.gov/ij/) by tracing their 2D contours on the photographs. Retraction was expressed as a percentage [(final clot size/initial clot size) × 100].

2.7 | Flow cytometry

Human washed platelets (30,000/µL), resting and activated by 50 µM ADP (Kordia), were incubated for 30 minutes at 37 °C with 570 nM Oregon Green 488 fibrinogen (Invitrogen), and with or without 25 µg/mL sEng (208 nM) in 25 µL of Tyrode's buffer, after which platelet-

bound Oregon green-fibrinogen was measured by flow cytometry using a BD Accuri C6 flow cytometer (BD Biosciences).

The expression of P-selectin and the binding of antiplatelet antibody PAC-1-FITC on platelets were assessed using washed platelets (3×10^8 platelets/mL) preincubated for 2 minutes with vehicle or sEng (5 μM), followed by incubation (without shaking) with PBS (resting) or TRAP6 (2 μM). After 5 minutes, diluted samples (1:10 in reacting buffer complemented with 0.3% BSA) were incubated with a mix of FITC-anti-CD62P (BD Pharmingen) and PE-anti-CD41 (Beckman Coulter) antibodies, or PAC-1-FITC (Becton Dickinson), or the corresponding irrelevant antibodies. After 10 minutes in the dark, samples were immediately analyzed using a BD Accuri flow cytometer. The results are expressed as the percentage of platelets expressing P-selectin or PAC-1 binding at the surface.

2.8 | Surface plasmon resonance binding analysis

The association between sEng-Strep-tag II [12] and integrin αIIbβ3 was analyzed by surface plasmon resonance (SPR) on a streptavidin (SA) biosensor (Cytiva) at 25 °C [50]. First, we immobilized 150 resonance units (RU) of sEng-Strep-tag II onto the test flow cell of a SA chip through the C-terminal StrepII tag to provide a sEng concentration on the surface of ~10 μM. The reference flow cell was not modified. Association was then tested in a single-cycle kinetics experiment by injecting increasing concentrations of purified integrin αIIbβ3 (R&D Systems #7148-A2-025 at 46.9, 93.8, 188, 375, and 750 nM) at 30 μL/min (contact time for the analyte or association time was 60 seconds) in 10 mM HEPES-NaOH (pH 7.4), 150 mM NaCl, and 0.01% (w/v) Polysorbate 20 (PS20), either supplemented with 1 mM $MnCl_2$ and 1 mM $CaCl_2$ or after extensive dialysis against EDTA to remove residual divalent cations in the protein preparation. Integrin αIIbβ3 (25 μg per experiment) was resuspended to 0.2 mg/mL (~1 μM) in the appropriate running buffer before use. Analysis was performed with the BiaEvaluation version 3.0.2 software (Cytiva) and the Anabel webserver (Analysis of binding events version 2.2.3; http://anabel.skscience.org/).

2.9 | Computational analysis

To access the atomistic details of the interaction between sEng and αIIbβ3, we used molecular modeling to generate complexes, as reported [51–59]. For the modeling of αIIbβ3, the well described active and inactive conformations of integrins were used [60,61], while for endoglin modeling, the reported dimeric structure was applied [51]. A more detailed description of this item can be found in the Methods and Supplementary Figure S2A–D.

2.10 | Transgenic mice

A mouse line overexpressing human sEng (amino acids 26-437) driven by a ubiquitous actin promoter on a CBAxC57BL/6J background

(hsEng+) was generated at the Genetically Modified Organisms Generation Unit of University of Salamanca, Spain, as previously described [9]. Progeny was screened for the endoglin transgene by PCR analysis of tail DNA. Studies reported here were performed in the F7 generation. The levels of human sEng in plasma were measured using a specific kit for human soluble endoglin (R&D Systems). Because these transgenic animals show variable levels of recombinant sEng in plasma, a minimum threshold of 1000 ng/mL of plasma sEng was established to include the mouse in the study group [9]. The average plasma levels of human sEng in the tested animals were ~1600 ng/mL, whereas those of control littermate mice were undetectable [9]. Compared with the levels of recombinant human sEng, the background levels of endogenous murine sEng were negligible (1-4 ng/mL), as previously described [20,62]. All animal procedures were conducted in strict compliance with the European Community Council Directive (2010/63/EU) and Spanish legislation (RD1201/2005 and RD53/2013). The protocols were approved by the University of Salamanca Ethical Committee.

2.11 | Bleeding time

To determine the tail bleeding time, hsEng+ and wild-type (WT) mice were disposed on a carpet with a constant temperature of 37 °C and anesthetized with isoflurane. Then, tails were transected at 3 mm from the tip and immediately immersed in PBS at 37 °C [5,63]. The time of the first cessation of bleeding was recorded, as well as the percentage of animals with rebleeding. The absence of rebleeding for 5 minutes was considered as cessation of bleeding, whereas mice that were still bleeding after 30 minutes were scored without arrest. For these latter mice, bleeding arrest was obtained by clamping the tail for 5 minutes.

2.12 | Hematologic analysis

Blood samples were obtained from the jugular vein of anesthetized mice in tubes containing 1 mM EDTA. Blood samples were centrifuged at 1600 g for 15 minutes at 4 °C, and plasma was collected. The concentration of human sEng was determined by Quantikine Human Eng/CD105 (R&D Systems). The prothrombin time and international normalized ratio (INR) were quantified using a portable coagulometer (INRatio 2, Alere). All the assays were performed on 24 mice (n = 12 WT and n = 12 hsEng+).

2.13 | Ferric chloride–induced thrombosis model in mice

$FeCl_3$-induced vascular injury is a widely used model of occlusive thrombosis that involves platelet activation and aggregation. This model is based on redox-induced endothelial cell injury [64]. Briefly, a 3-cm incision was made in the mouse neck, and the carotid artery was

isolated from the surrounding tissues. Then, a filter paper (1 × 2 mm) soaked in $FeCl_3$ solution (7.5%) was topically deposited for 90 seconds on the carotid artery, and the flux and thrombus formation were monitored in real-time using a Transonic probe (Transonic Systems Inc). Carotid occlusion due to thrombus formation led to a decrease in blood flow. Throughout the experiment, recoveries in blood flow of >20% with respect to the background levels were recorded to determine the number of released emboli in each mouse (Supplementary Figure S3).

2.14 | Statistics

Data were subjected to statistical analysis, and the results are shown as mean ± SD. Normality was analyzed with the Shapiro-Wilk test. When the test did not indicate normality (data in Figures 1 and 5), we performed a nonparametric analysis using the Mann-Whitney test. Otherwise, 2-group comparison was performed with parametric Student's t-test, and multiple comparisons were done by 1-way (one variable) or 2-way (2 variables) ANOVA. In addition, Fisher's exact test was used for the comparison of proportions when necessary.

3 | RESULTS

3.1 | sEng reduces thrombus formation under flow conditions in vitro

The effect of sEng on thrombus formation was tested *in vitro* under flow conditions using human whole blood supplemented or not with sEng (5 µg/mL) and perfused on collagen-coated chambers at a shear rate of 56 dynes/cm^2. As shown in Figure 1A (Supplementary Videos S1 and S2), sEng did not prevent the initial adhesion of platelets to collagen but decreased the size of the aggregates. Indeed, in the presence of sEng, aggregates were smaller than in the control (mean: 40 µm vs 350 µm; *P < .05; Figure 1B). Similar results were obtained by using 1 µg/mL sEng (*P < .05; Supplementary Figure S4).

3.2 | sEng inhibits platelet aggregation and clot retraction

Human washed platelets, preincubated with vehicle or various concentrations of sEng, were activated by TRAP6, and aggregation was monitored in microplates as reported [65]. Compared to vehicle-treated platelets, TRAP6 at 1 µM induced a strong aggregation, which reached, at least, 80% with all donors tested. sEng alone did not induce platelet aggregation at the concentrations used (Figure 2A). On the contrary, sEng induced a dose-dependent inhibition of TRAP6-induced aggregation that was statistically significant at 1 µg/mL (*P < .05) of sEng and reached 50% inhibition at 5 µg/mL sEng (**P < .01; Figure 2A–C). To rule out that the sEng-induced inhibition of aggregation was not restricted to TRAP6-induced activation, the
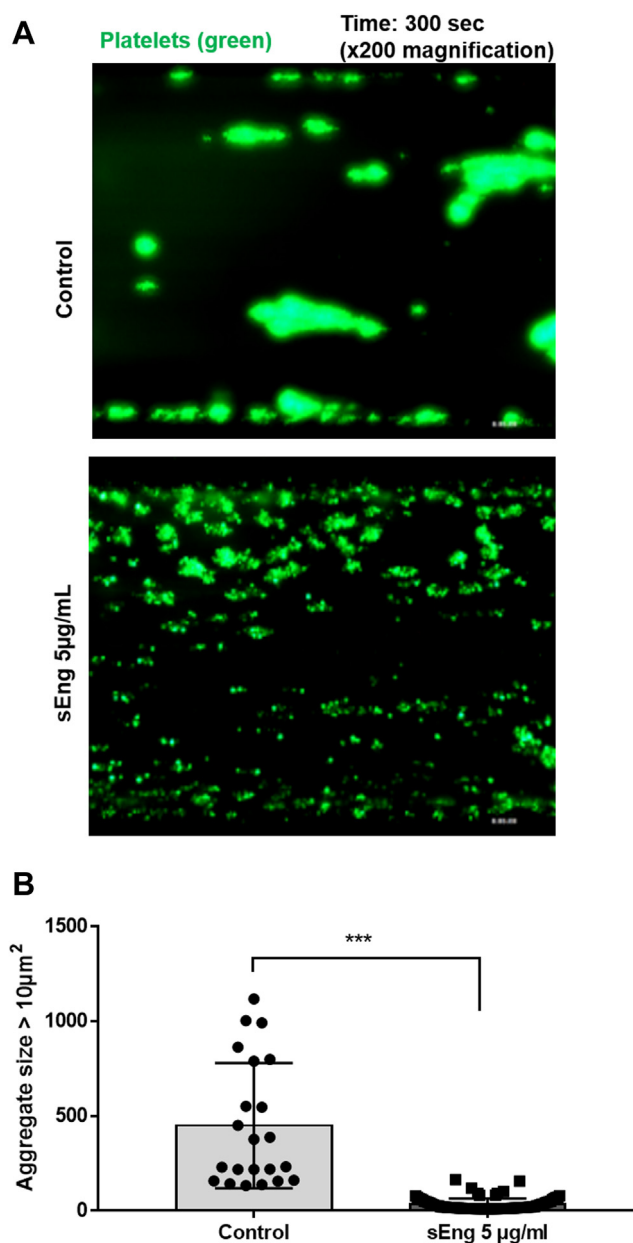

A Platelets (green)   Time: 300 sec (x200 magnification)

Control

sEng 5µg/mL

B

FIGURE 1 Effect of sEng on human platelet aggregation. Total blood was stained with calcein and loaded on collagen-coated chambers and preincubated with vehicle (control) or sEng (5 µg/mL). Then, perfusion was carried out for 5 minutes (300 seconds) and platelets were visualized by green fluorescence microscopy. (A) Perfusion performed in the presence of sEng resulted in smaller and more disperse aggregates compared to controls. Images are representative of 5 separate experiments (magnification, ×200). (B) Quantification of each aggregate area obtained at the end of the perfusion and corresponding to 5 different donors showed that sEng-treatment (5 µg/mL) resulted in the formation of more numerous aggregates of smaller size compared to control (***P < .001). Indeed, control aggregates frequently reached a size of >300 µm^2, whereas in the presence of sEng, platelets remained dispersed and barely formed aggregates larger than the cutoff (10 µm^2).

experiment was reproduced using the thromboxane-prostanoid (TP)–receptor agonist U46619 (0.5 µM). As in the case of TRAP6 activation, the strong aggregation (>90%) induced by U46619 was
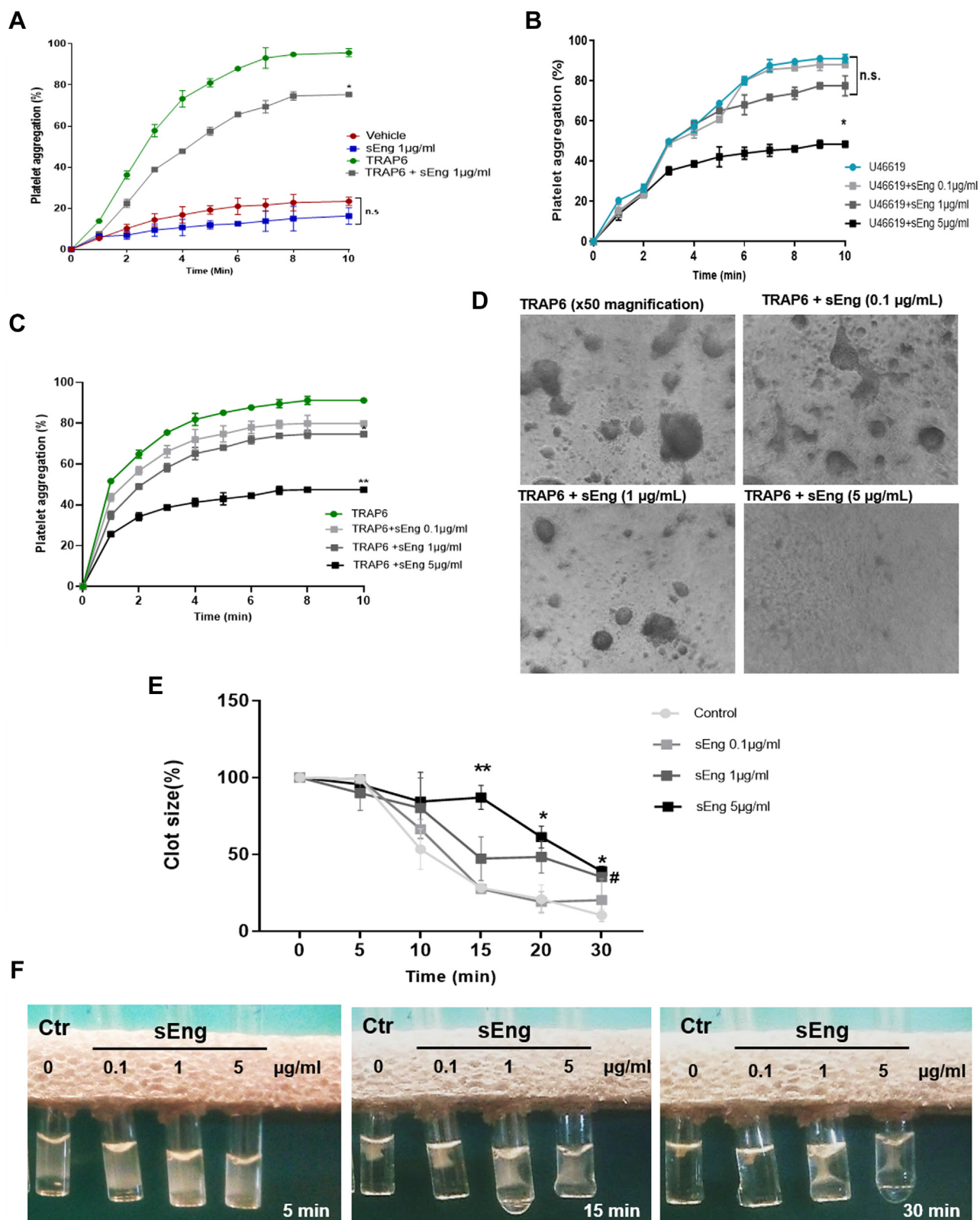
FIGURE 2 Platelet aggregation in microplates and thrombus retraction are inhibited by sEng. (A–C) Human washed platelets (3×10^8 platelets/mL) were preincubated with vehicle or sEng (0.1, 1, or 5 µg/mL) before addition of 1 µM TRAP6. Aggregations were measured under stirring in a microplate reader set at 37 °C. (A) Aggregation kinetics with buffer, sEng, TRAP6, and sEng+TRAP6. The graph shows that sEng is not able to induce platelet aggregation. (B, C) Aggregation kinetics with different concentrations of sEng and quantification of n = 10 different donors at 10-minute time-point using U46619 (0.5 µM) and TRAP6 (1 µM), respectively. A significant reduction of aggregation was observed at 1 µg/mL of sEng (*$P < .05$) and 5 µg/mL of sEng (**$P < .01$). (D) Representative images of platelet aggregates, as visualized by optical microscopy

significantly reduced with 5 µg/mL sEng (*$P < .05$; Figure 2B). The inhibition of aggregation was also observed by the disappearance of large aggregates in suspension at the end of the reaction (Figure 2D). These results were confirmed using the reference technique of optical aggregometry (Supplementary Figure S5A–C). To evaluate clot retraction, thrombin and Ca^{2+} were added to washed platelets supplemented with fibrinogen in the presence of various concentrations of sEng (0.1 µg/mL, 1 µg/mL, or 5 µg/mL; Figure 2E, F). Photos were taken every 5 minutes from 0 to 30 minutes. At 15 minutes, a significantly impaired clot retraction was observed in the presence of 5 µg/mL of sEng compared to control (without sEng), with mean retraction values of 10% vs 70%, respectively (*$P < .05$; Figure 2E). Clot retraction impairment was also significant with 1 µg/mL of sEng at 30 minutes (*$P < .05$; Figure 2E).

3.3 | sEng does not interfere with platelet activation, but interacts with αIIbβ3 preventing fibrinogen binding

To determine whether the inhibitory activity of sEng was specific to platelet aggregation and had no direct effect on platelet activation, we next examined the impact of sEng on platelet secretion. We found that sEng decreased the binding of PAC-1 (a monoclonal antibody that specifically recognized activated integrin αIIbβ3) with platelets activated by TRAP6 (Figure 3A; $P < .01$), likely by acting on the αIIbβ3 complex. Interestingly, under the same condition, the percentage of positive platelets for P-selectin (a marker of platelet secretion) was not modified in the presence of sEng (Figure 3B). This lack of modulatory activity of sEng on secretion suggests that sEng does not affect platelet activation but possibly PAC-1 binding to integrin. To further test the hypothesis that sEng inhibits aggregation by direct interaction with αIIbβ3, a competition assay between sEng and Oregon Green 488–labeled fibrinogen on resting or activated platelets was performed. As expected, ADP, a weak platelet agonist, induced activation of αIIbβ3 and thus fibrinogen binding, whereas sEng significantly decreased this binding (Figure 3C; $P < .01$).

3.4 | Experimental and computational analysis of the interaction between Eng and integrin αIIbβ3

Taken together, the above results suggest that the modulatory effects of sEng on hemostasis could be mediated by its interaction with the integrin αIIbβ3, which is expressed at high levels in platelets. To investigate this interaction, we analyzed the association between sEng-Strep-tag II (sEng-Strep) and integrin αIIbβ3 by surface plasmon resonance (SPR) on a streptavidin (SA) biosensor (Cytiva) at 25 °C using single-cycle kinetics. When nonactivated integrin αIIbβ3 was flowed over surface-immobilized sEng-Strep, no binding was detected (Figure 4A, light blue line). In contrast, when activated Ca^{2+}/Mn^{2+}-loaded integrin αIIbβ3 was flowed instead, the first (46.9 nM) and second (93.8 nM) injections showed fast binding and slow dissociation phases, which allowed the estimation of approximate binding parameters (Figure 4A, dark blue line). The second injection already accomplished 100% binding saturation at 168 RU (maximum theoretical RU = 150 RU). Apparent association ($k_{on} = 0.052 ± 0.002$ $M^{-1} s^{-1}$) and dissociation ($k_{off} < 0.008$ s^{-1}) kinetic constants were estimated from the complete single-cycle kinetics experiment or the first injection only, and used to estimate the apparent equilibrium dissociation constant K_D of <9 nM. At greater concentrations of integrin αIIbβ3 (>100 nM), binding either plateaued, indicating binding saturation on the SA chip, or was artificially reduced through nonspecific binding to the reference flow cell.

The above data demonstrate the direct interaction between sEng and integrin αIIbβ3, and this association was further analyzed *in silico*. Docking analysis showed that sEng and active (open conformation) or inactive (closed conformation) integrin αIIbβ3 could form low energy stable complexes (Figure 4B). As detailed in the method section, we discarded all hits that were not physically relevant because the interaction surface or the number of contact residues was too small to yield a plausible stable docking. Moreover, we analyzed the details of the contact regions, focusing on those for which there was a true penetration of 1 chain into the other and establishing a relevant number of contacts. We first focused on the complex formed by active αIIbβ3 as this form is the one that typically interacts with fibrinogen. We found several possible stable complexes and large clusters of structures exhibiting a direct interaction between one of the RGD motifs of sEng and αIIbβ3 (Figure 4B [left structure] and Supplementary Videos S3 and S4). In this condition, the position occupied by RGD is at the interface between αIIb and β3, in the same region where fibrinogen binds (as shown in the crystal structure PDB ID: 2VDO [56]). Next, we also investigated the possible interaction between sEng and the closed conformation of inactive αIIbβ3. When looking at the sEng+inactive integrin complex, we found structures with just 1 arm of sEng engaged in interaction with αIIbβ3, whereas the other arm remained free of contacts (Figure 4B, right structure). Overall, our *in silico* predictions of a more stable complex between sEng and the activated αIIbβ3 compared to the complex formed with the inactivated αIIbβ3, are in agreement with the strong vs lack of interaction, respectively, detected by SPR (Figure 4A).

after 10 minutes (magnification, ×50). (E, F) Clot retraction was studied from 0 to 30 minutes after adding thrombin and Ca^{2+} to washed platelets maintained at 37 °C with fibrinogen (0.5 mg/mL) in the presence or absence (control) of various concentrations of sEng. (E) Kinetic analysis of the retraction experiment expressed as a percentage of the clot size at time 0 (n = 5 different donors; control vs 5 µg/mL of sEng at 15 minutes, **$P < .01$; control vs 5 µg/mL of sEng at 20 and 30 minutes, *$P < .05$; control vs 1 µg/mL of sEng at 30 minutes, #$P < .05$). (F) Representative images of clot retraction at 5, 15, and 30 minutes after the addition of thrombin. n.s., not significant.
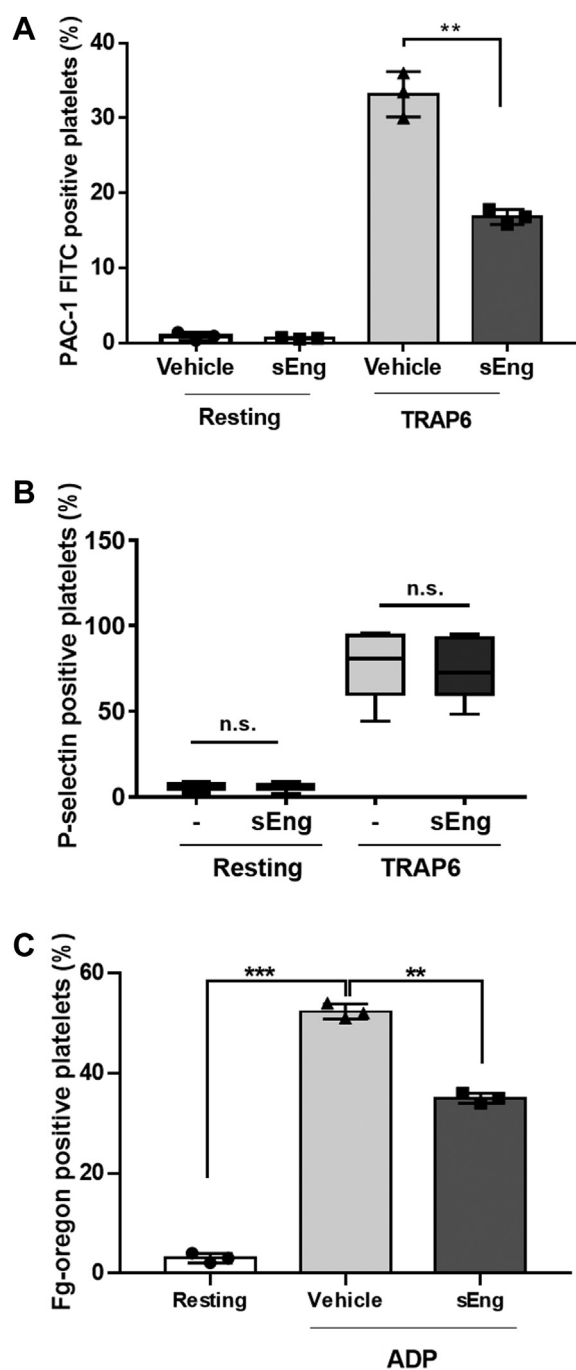
FIGURE 3 sEng does not interfere with platelet activation, but interacts with αIIbβ3, preventing PAC-1 and fibrinogen binding. Human washed platelets, resting or activated by 2 μM TRAP6 or 50 μM ADP, were treated with or without sEng (25 μg/mL = 208 nM), as indicated. Then, samples were incubated with FITC-conjugated PAC-1 (A), a mix of FITC-conjugated anti-CD62 (anti-P-selectin) and PE-conjugated anti-CD41 antibodies (to determine total platelets) (B), or with Oregon Green 488 fibrinogen (C). All samples were analyzed by flow cytometry using a BD Accuri C6 flow cytometer (BD Biosciences). The percentage of positive platelets is displayed in each case. n = 6; **$P < .01$; ***$P < .001$. n.s., not significant.

3.5 | sEng regulates bleeding and thrombus formation in mice

To confirm the role of sEng in hemostasis, we analyzed bleeding parameters and thrombus formation using a previously reported transgenic mouse line that overexpresses human sEng (hsEng+) [9]. There were no differences between hsEng+ and WT mice in terms of hematology parameters such as platelet count (data not shown). We observed that hsEng+ mice had significantly longer bleeding times, either considering the first cessation of bleeding (Figure 5A) or total bleeding (bleeding + rebleeding), since at 30 minutes, 10 out of 12 hsEng+ mice continued to bleed compared with 2 out of 10 for the WT (*$P < .05$; Figure 5B). Furthermore, we found that the number of animals undergoing rebleeding was significantly higher in hsEng+ mice than in controls (*$P < .05$; Figure 5C). In addition, the total number of rebleeding per mouse was markedly increased in hsEng+ mice compared to control animals (*$P < .05$; Figure 5D). In addition, no significant difference existed in prothrombin time or international normalized ratio (INR) between hsEng+ and WT mice (Figure 5E, F). The impact of increased concentrations of sEng on hemostasis was also evaluated in vivo using a model of carotid artery thrombosis. Thus, hsEng+ mice showed a significantly longer time to occlusion than WT (500 ± 147 vs 388 ± 103 seconds, respectively; $P < .05$; Figure 5G). Moreover, the thrombus appeared less stable as suggested by more frequent emboli in hsEng+ mice compared to WT, either considering the number of emboli per mouse (mean 1.6 ± 0.8 vs 0.5 ± 0.5, respectively; $P = .01$; Figure 5H) or the number of mice that had at least 1 embolic event. Indeed, the analysis of full flow recovery after partial closure showed that 38% of WT animals presented at least 1 reopening event after partial closure and this percentage increased to 78% in hsEng+ mice, suggesting that thrombi are less stable in hsEng+ than in WT mice. Taken together, these results support the potential effect of sEng on primary hemostasis in vivo.

4 | DISCUSSION

This study demonstrates that sEng interferes with thrombus formation and stabilization. Thrombus formation is mediated by αIIbβ3 that, on resting platelets, is in an inactive conformation with a low affinity for fibrinogen. Following platelet activation, αIIbβ3, switching from low affinity (resting) to high affinity (active) state for ligand binding [66], thus acquires its platelet aggregation receptor activity, resulting in its key role in hemostasis [67]. Recently, we reported the interaction between membrane endoglin of endothelial cells and platelets, involving the endoglin RGD motif [5] and the activated αIIbβ3 of human and murine platelets [68]. Furthermore, in vitro experiments using human Eng mutated on the RGD sequence (ie, RGA) supported the role of this motif in the Eng-integrin interaction [43]. Since sEng encompasses the extracellular region of membrane endoglin, including the RGD motif, we hypothesized that sEng is able to bind integrin

FIGURE 4 Surface plasmon resonance analysis and modeling (docking) of endoglin and integrin αIIbβ3 interactions. (A) Binding analysis of sEng-Strep-tag II (sEng-Strep) and integrin αIIbβ3 by surface plasmon resonance. Top: sensorgram corresponding to the first 2 consecutive injections of the ligand (integrin αIIbβ3) over the streptavidin sensor chip immobilized with sEng-Strep. The concentration of integrin αIIbβ3 at each injection is indicated. Binding association (k_{on}) and dissociation (k_{off}) phases are shown by arrows. Bottom: apparent kinetic and equilibrium dissociation binding parameters for the interaction calculated by nonlinear regression. (B) Structural modeling of the complex between active (left) and inactive (right) integrin αIIbβ3 (dark-light blue) and sEng (dark-light pink). The shaded area indicates the surface of the molecules computed from the positions of all atoms. The atoms in contact between the 2 molecules are highlighted with spheres, and the sEng RGD motif is marked in red.

k_{on} $(M^{-1} s^{-1})$	k_{off} (s^{-1})	K_D (nM)
0.052 ± 0.002	< 0.008	< 9
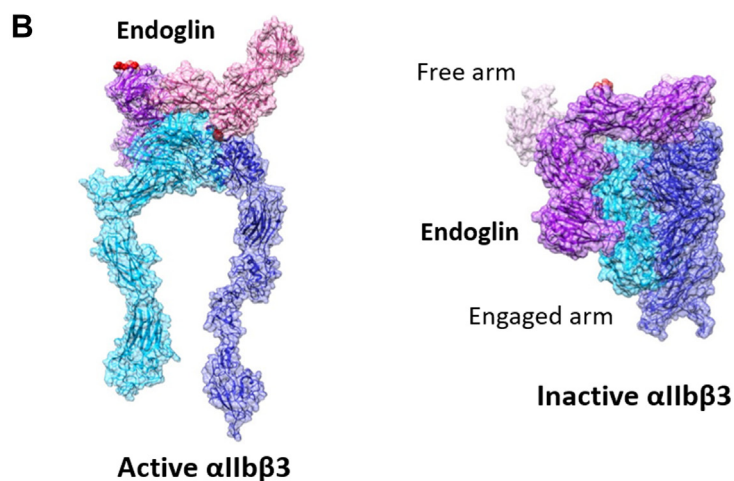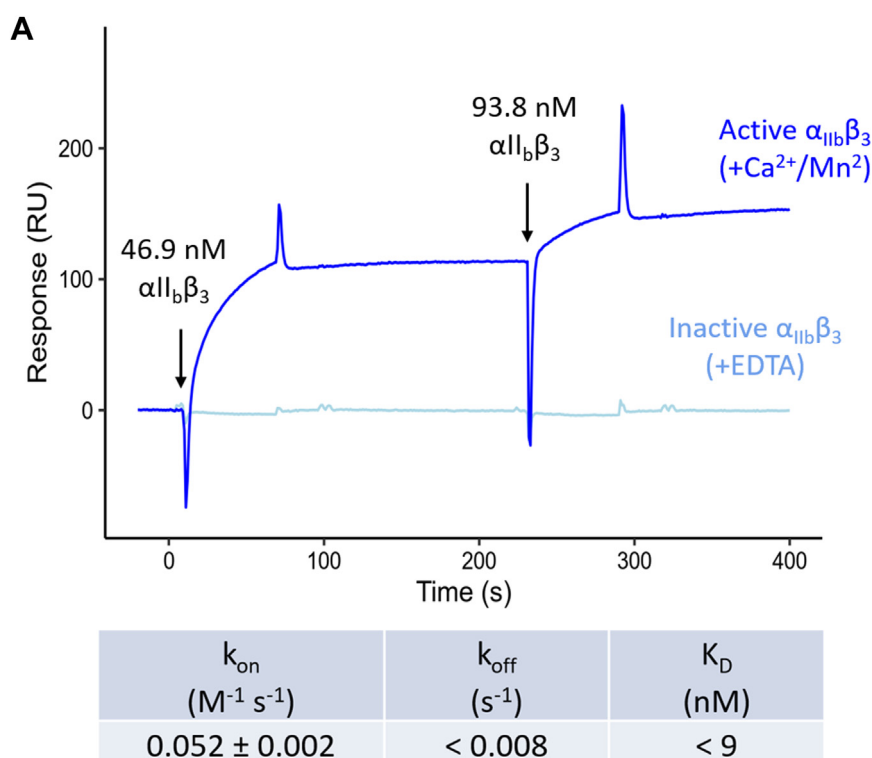
αIIbβ3 in humans as well as in mice, which entails a series of consequences. Our present study supports this hypothesis since the data demonstrate that sEng intervenes in platelet aggregation, acting as a competitor of fibrinogen during clot formation. This is in agreement with the tight K_D value ($K_D < 9$ nM) of the sEng/αIIbβ3 interaction compared with that of fibrinogen/αIIbβ3 ($K_D = 50$ nM), both measured using the same SPR technique [69]. Indeed, using whole blood aggregation assays under flow conditions, we found that sEng reduced aggregation stimulated by strong agonists, such as TRAP6 and the TP-receptor agonist U46619, or a weak agonist such as ADP, without affecting platelet activation, as suggested by its absence of effect on platelet secretion.

Clot retraction, allowing the stabilization of the aggregates, is the final step during platelet activation, which involves the binding of fibrinogen to αIIbβ3 and consequently the outside-in signaling pathways that induce cytoskeletal rearrangement necessary for the retraction. Platelets pull on fibrin strands to consolidate the hemostatic plug and to further allow the blood circulation [70]. Therefore, we also evaluated thrombus retraction in the presence of sEng, providing evidence that sEng delays clot retraction. The inhibitory effect of sEng on ligand binding to αIIbβ3 is also supported by our *in vitro* assays, which demonstrated that sEng binds platelets after stimulation and interferes with fibrinogen and PAC-1 binding without affecting platelet activation.
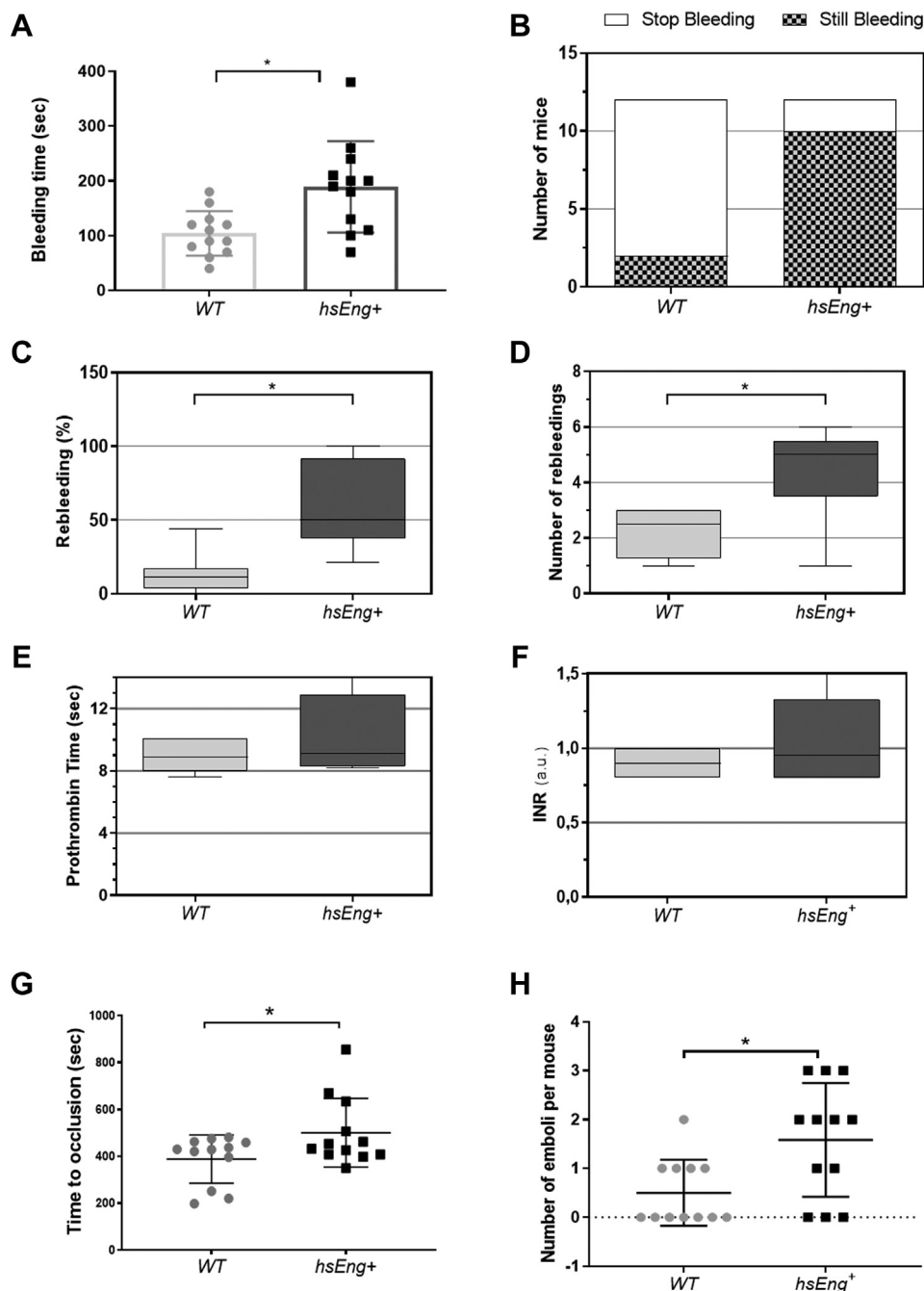
FIGURE 5 **Hemostasis assays in WT and *hsEng*+ mice.** (A) Tail bleeding time, corresponding to the first cessation of bleeding, in WT (n = 12) and *hsEng*+ mice (n = 12; *P < .05). (B) Final bleeding. At the end of the experiment (after 30 minutes), 2 out of 12 WT animals stopped bleeding, whereas 10 out of 12 *hsEng*+ mice were still bleeding (0.166 vs 0.833 ratios, respectively; P = .0033 according to Fisher's exact test). (C) In *hsEng*+ mice, 60% of animals showed rebleeding vs 20% of WT mice (*P < .05). (D) The number of rebleedings in *hsEng*+ mice was twice that of controls (*P < .05). No significant differences were found between WT and *hsEng*+ mice considering prothrombin time (E) or the INR (F). (G, H) Thrombus formation after FeCl$_3$ administration on carotid artery. (G) Time to final occlusion (blood flow arrest) in WT (n = 12) and *hsEng*+ (n = 12) mice (*P < .05). (H) A higher number of emboli per mice were found in *hsEng*+ mice compared to control animals (*P < .05). a.u., arbitrary units; INR, international normalized ratio.

A two-step mechanism for αIIbβ3 binding to fibrinogen has been suggested: the γ sequence of fibrinogen itself is able to initiate αIIbβ3 clustering and recruitment of intracellular proteins to early focal complexes, mediating cell attachment, while the RGD motif (on the α chain) subsequently acts as a molecular switch on the β3 subunit to trigger cell spreading [71]. Figure 6 illustrates our hypothesis that sEng inhibits platelet aggregation and induces a destabilization of thrombus by preventing or interfering with fibrinogen-αIIbβ3 bridges. Supporting the involvement of sEng in this process, SPR and computational analyses showed that the sEng-αIIbβ3 interaction
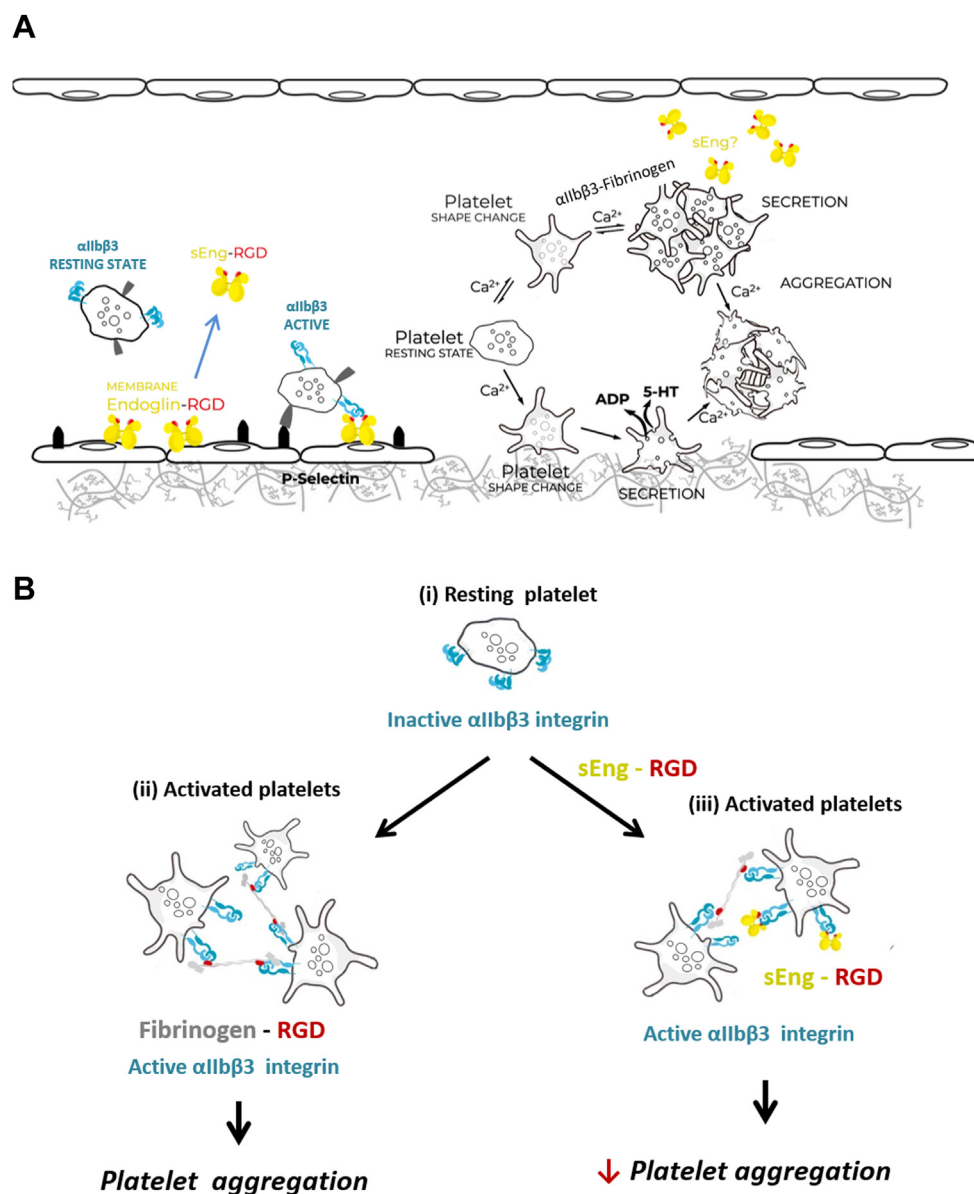
FIGURE 6 Hypothetical mechanism of sEng-induced inhibition of platelet aggregation. (A) Hemostasis is triggered upon vascular injury to seal off the damage. During the initial phase, circulating platelets are recruited to the injury site via adhesive interactions, including the binding between membrane-bound endothelial endoglin and platelet αIIbβ3 [5]. Upon activation by a variety of stimuli, platelets undergo secretion and aggregation to one another involving integrin αIIbβ3–mediated interactions of platelets with fibrinogen. Membrane-bound endoglin can be proteolytically processed to yield a soluble form of endoglin (sEng) that contains an RGD motif. (B) Resting platelets expose inactive integrin αIIbβ3 on their surface (i), but after platelet stimulation, integrin αIIbβ3 is activated, enabling the formation of fibrinogen-αIIbβ3 interactions mediated by the RGD motif leading to platelet aggregation (ii). sEng binds to αIIbβ3 via its RGD motif, inducing a destabilization of the thrombus by "interfering" with fibrinogen-αIIbβ3 interactions and thus inhibiting platelet aggregation. The RGD motif is highlighted in red.

occurs when the integrin is in its active form, but not in its inactive form.

The inhibitory effect of sEng was also confirmed *in vivo*. Indeed, we showed that mice overexpressing sEng (*hsEng*+) and displaying a range of circulating endoglin concentrations between 1 and 5 μg/mL bled more than WT and presented more rebleeding and impairment in bleeding arrest even after 30 minutes, although no anomalies in coagulation factor levels were observed. Furthermore, after inducing thrombus formation, we found that artery occlusion lasted longer and

was less stable in *hsEng*+ than in control mice, suggesting that sEng circulating in h*sEng*+ mice was implicated in clot formation and stabilization.

Integrin αIIbβ3 is a target of potent antiplatelet agents such as eptifibatide, tirofiban, and abciximab. However, due to the associated high bleeding risk, their use is currently limited to acute settings such as during percutaneous coronary intervention or acute coronary syndrome in patients with high thrombotic risk [72]. Therefore, there is a current need to find alternative, antiplatelet, and safer drugs [73].

In this context, our results propose that Eng is a physiological ligand of αIIbβ3, and open a new research avenue to study sEng as an anti-platelet drug agent. All in all, our data highlight a beneficial and potential interest of sEng to not only prevent platelet binding to fibrinogen, impairing aggregation and stability of the thrombus, but also identify and target platelets with sEng for new therapeutic approaches.

In summary, we described for the first time the potential significance of the interaction between sEng and αIIbβ3 integrin in the thromboinflammatory context. This pathophysiological context is controlled by αIIbβ3, which is a platelet-specific integrin that plays a key role in platelet functions, namely, platelet aggregation, which is a central response in hemostasis and thrombosis. Accordingly, by binding to the αIIbβ3 integrin, sEng could regulate platelet functions. Further studies are needed to better understand the pathophysiological relevance of the sEng/αIIbβ3 interaction and its potential therapeutic applications.

AUTHOR CONTRIBUTIONS

E.R. designed and supervised the research, analyzed the data, and wrote the paper. M.P. and L.G.-P. performed in vivo assays. E.R., A.K., C.B.-L., A.L., C.E.-T., D.E.H., and A.M. performed in vitro assays. E.R. and S.P. performed and analyzed the in silico data. F.J.F. and M.C.V. performed and analyzed the SPR experiments. P.G., I.M., D.M.S., C.B.-L., and C.B. provided useful suggestions for the development of this study. E.R., C.B.-L., M.C.V., and C.B. interpreted and discussed the results, revised the paper, and provided funding support. All authors read and approved the final paper.

DECLARATION OF COMPETING INTEREST

A patent titled "Methods and pharmaceutical composition for treating thrombotic disorders" (EP22305156) related to soluble endoglin and supported by INSERM Transfert (Institut National de la Santé et de la Recherche Médicale) has been granted to E.R. A review on "Novel vascular roles of endoglin" was presented in the "State-of-the-art" session by E.R. at the 30th Congress of the International Society on Thrombosis and Haemostasis (ISTH) in London, UK (July 9, 2022, to July 13, 2022).

ORCID

Elisa Rossi https://orcid.org/0000-0002-0570-6104
Miguel Pericacho https://orcid.org/0000-0003-0226-482X
Alexandre Kauskot https://orcid.org/0000-0002-4064-8114
Luis Gamella-Pozuelo https://orcid.org/0000-0003-3556-2495
Etienne Reboul https://orcid.org/0000-0003-0759-4756
Alexandre Leuci https://orcid.org/0000-0001-9329-8165
Divina El Hamaoui https://orcid.org/0000-0003-1384-1207
Aurore Marchelli https://orcid.org/0000-0002-8638-306X
Francisco J. Fernández https://orcid.org/0000-0002-5015-1849
Isabelle Margaill https://orcid.org/0000-0002-7941-6644
M. Cristina Vega https://orcid.org/0000-0003-0628-8378
Pascale Gaussem https://orcid.org/0000-0002-9139-2147
Samuela Pasquali https://orcid.org/0000-0003-1487-0894
David M. Smadja https://orcid.org/0000-0001-7731-9202
Christilla Bachelot-Loza https://orcid.org/0000-0002-6264-902X
Carmelo Bernabeu https://orcid.org/0000-0002-1563-6162

REFERENCES

[1] López-Novoa JM, Bernabeu C. The physiological role of endoglin in the cardiovascular system. *Am J Physiol Heart Circ Physiol*. 2010;299: H959–74.

[2] Shovlin CL. Hereditary haemorrhagic telangiectasia: pathophysiology, diagnosis and treatment. *Blood Rev*. 2010;24:203–19.

[3] Faughnan ME, Mager JJ, Hetts SW, Palda VA, Lang-Robertson K, Buscarini E, Deslandres E, Kasthuri RS, Lausman A, Poetker D, Ratjen F, Chesnutt MS, Clancy M, Whitehead KJ, Al-Samkari H, Chakinala M, Conrad M, Cortes D, Crocione C, Darling J, et al. Second international guidelines for the diagnosis and management of hereditary hemorrhagic telangiectasia. *Ann Intern Med*. 2020;173: 989–1001.

[4] Faughnan ME, Palda VA, Garcia-Tsao G, Geisthoff UW, McDonald J, Proctor DD, Spears J, Brown DH, Buscarini E, Chesnutt MS, Cottin V, Ganguly A, Gossage JR, Guttmacher AE, Hyland RH, Kennedy SJ, Korzenik J, Mager JJ, Ozanne AP, Piccirillo JF, et al. International guidelines for the diagnosis and management of hereditary haemorrhagic telangiectasia. *J Med Genet*. 2011;48:73–87.

[5] Rossi E, Pericacho M, Bachelot-Loza C, Pidard D, Gaussem P, Poirault-Chassac S, Blanco FJ, Langa C, González-Manchón C, Novoa JML, Smadja DM, Bernabeu C. Human endoglin as a potential new partner involved in platelet–endothelium interactions. *Cell Mol Life Sci*. 2018;75:1269–84.

[6] Egido-Turrión C, Rossi E, Ollauri-Ibáñez C, Pérez-García ML, Sevilla MA, Bastida JM, González-Porras JR, Rodríguez-Barbero A, Bernabeu C, Lopez-Novoa JM, Pericacho M. Functional alterations involved in increased bleeding in hereditary hemorrhagic telangiectasia mouse models. *Front Med (Lausanne)*. 2022;9:871903.

[7] Ruiz-Llorente L, Gallardo-Vara E, Rossi E, Smadja DM, Botella LM, Bernabeu C. Endoglin and alk1 as therapeutic targets for hereditary hemorrhagic telangiectasia. *Expert Opin Ther Targets*. 2017;21:933–47.

[8] Hawinkels LJAC, Kuiper P, Wiercinska E, Verspaget HW, Liu Z, Pardali E, Sier CF, ten Dijke P. Matrix metalloproteinase-14 (MT1-MMP)-mediated endoglin shedding inhibits tumor angiogenesis. *Cancer Res*. 2010;70:4141–50.

[9] Valbuena-Diez AC, Blanco FJ, Oujo B, Langa C, Gonzalez-Nuñez M, Llano E, Pendas AM, Díaz M, Castrillo A, Lopez-Novoa JM, Bernabeu C. Oxysterol-induced soluble endoglin release and its involvement in hypertension. *Circulation*. 2012;126:2612–24.

[10] Aristorena M, Gallardo-Vara E, Vicen M, de Las Casas-Engel M, Ojeda-Fernandez L, Nieto C, Blanco FJ, Valbuena-Diez AC,

Botella LM, Nachtigal P, Corbi AL, Colmenares M, Bernabeu C. MMP-12, secreted by pro-inflammatory macrophages, targets endoglin in human macrophages and endothelial cells. *Int J Mol Sci.* 2019;20:3107.

[11] Letarte M, McDonald ML, Li C, Kathirkamathamby K, Vera S, Pece-Barbara N, Kumar S. Reduced endothelial secretion and plasma levels of transforming growth factor-beta1 in patients with hereditary hemorrhagic telangiectasia type 1. *Cardiovasc Res.* 2005;68:155–64.

[12] Perucci LO, Gomes KB, Freitas LG, Godoi LC, Alpoim PN, Pinheiro MB, Miranda AS, Teixeira AL, Dusse LM, Sousa LP. Soluble endoglin, transforming growth factor-Beta 1 and soluble tumor necrosis factor alpha receptors in different clinical manifestations of preeclampsia. *PloS One.* 2014;9:e97632.

[13] Botella LM, Albiñana V, Ojeda-Fernandez L, Recio-Poveda L, Bernabéu C. Research on potential biomarkers in hereditary hemorrhagic telangiectasia. *Front Genet.* 2015;6:115.

[14] Rana S, Burke SD, Karumanchi SA. Imbalances in circulating angiogenic factors in the pathophysiology of preeclampsia and related disorders. *Am J Obstet Gynecol.* 2022;226:S1019–34.

[15] Rios DRA, Alpoim PN, Godoi LC, Perucci LO, de Sousa LP, Gomes KB, Dusse LMS. Increased levels of sENG and sVCAM-1 and decreased levels of VEGF in severe preeclampsia. *Am J Hypertens.* 2016;29:1307–10.

[16] Leaños-Miranda A, Navarro-Romero CS, Sillas-Pardo LJ, Ramírez-Valenzuela KL, Isordia-Salas I, Jiménez-Trejo LM. Soluble endoglin as a marker for preeclampsia, its severity, and the occurrence of adverse outcomes. *Hypertension.* 2019;74:991–7.

[17] Margioula-Siarkou G, Margioula-Siarkou C, Petousis S, Margaritis K, Vavoulidis E, Gullo G, Alexandratou M, Dinas K, Sotiriadis A, Mavromatidis G. The role of endoglin and its soluble form in pathogenesis of preeclampsia. *Mol Cell Biochem.* 2022;477:479–91.

[18] Venkatesha S, Toporsian M, Lam C, Hanai J, Mammoto T, Kim YM, Bdolah Y, Lim KH, Yuan HT, Libermann TA, Stillman IE, Roberts D, D'Amore PA, Epstein FH, Sellke FW, Romero R, Sukhatme VP, Letarte M, Karumanchi SA. Soluble endoglin contributes to the pathogenesis of preeclampsia. *Nat Med.* 2006;12:642–9.

[19] Gallardo-Vara E, Gamella-Pozuelo L, Perez-Roque L, Bartha JL, Garcia-Palmero I, Casal JI, López-Novoa JM, Pericacho M, Bernabeu C. Potential role of circulating endoglin in hypertension via the upregulated expression of BMP4. *Cells.* 2020;9:988.

[20] Pérez-Roque L, Núñez-Gómez E, Rodríguez-Barbero A, Bernabéu C, López-Novoa JM, Pericacho M. Pregnancy-induced high plasma levels of soluble endoglin in mice lead to preeclampsia symptoms and placental abnormalities. *Int J Mol Sci.* 2020;22:165.

[21] Víšek J, Bláha M, Bláha V, Lášticová M, Lánska M, Andrýs C, Tebbens JD, Igreja ESá IC, Tripská K, Vicen M, Najmanová I, Nachtigal P. Monitoring of up to 15 years effects of lipoprotein apheresis on lipids, biomarkers of inflammation, and soluble endoglin in familial hypercholesterolemia patients. *Orphanet J Rare Dis.* 2021;16:110.

[22] Vicen M, Igreja Sá IC, Tripská K, Vitverová B, Najmanová I, Eissazadeh S, Micuda S, Nachtigal P. Membrane and soluble endoglin role in cardiovascular and metabolic disorders related to metabolic syndrome. *Cell Mol Life Sci.* 2021;78:2405–18.

[23] Blázquez-Medela AM, García-Ortiz L, Gómez-Marcos MA, Recio-Rodríguez JI, Sánchez-Rodríguez A, López-Novoa JM, Martínez-Salgado C. Increased plasma soluble endoglin levels as an indicator of cardiovascular alterations in hypertensive and diabetic patients. *BMC Med.* 2010;8:86.

[24] Ceriello A, La Sala L, De Nigris V, Pujadas G, Testa R, Uccellatore A, Genovese S. GLP-1 reduces metalloproteinase-14 and soluble endoglin induced by both hyperglycemia and hypoglycemia in type 1 diabetes. *Endocrine.* 2015;50:508–11.

[25] Emeksiz HC, Bideci A, Damar Ç, Derinkuyu B, Çelik N, Döğer E, Yüce Ö, Özmen MC, Çamurdan MO, Cinaz P. Soluble endoglin level

[26] Malik RA, Li C, Aziz W, Olson JA, Vohra A, McHardy KC, Forrester JV, Boulton AJ, Wilson PB, Liu D, McLeod D, Kumar S. Elevated plasma CD105 and vitreous VEGF levels in diabetic retinopathy. *J Cell Mol Med.* 2005;9:692–7.

[27] Tomášková V, Mýtniková A, Hortová Kohoutková M, Mrkva O, Skotáková M, Šitina M, Helánová K, Frič J, Pařenica J, Šrámek V, Helán M. Prognostic value of soluble endoglin in patients with septic shock and severe COVID-19. *Front Med (Lausanne).* 2022;9:972040.

[28] Li CG, Bethell H, Wilson PB, Bhatnagar D, Walker MG, Kumar S. The significance of CD105, TGFbeta and CD105/TGFbeta complexes in coronary artery disease. *Atherosclerosis.* 2000;152:249–56.

[29] Ikemoto T, Hojo Y, Kondo H, Takahashi N, Hirose M, Nishimura Y, Katsuki T, Shimada K, Kario K. Plasma endoglin as a marker to predict cardiovascular events in patients with chronic coronary artery diseases. *Heart Vessels.* 2012;27:344–51.

[30] Saita E, Miura K, Suzuki-Sugihara N, Miyata K, Ikemura N, Ohmori R, Ikegami Y, Kishimoto Y, Kondo K, Momiyama Y. Plasma soluble endoglin levels are inversely associated with the severity of coronary atherosclerosis-brief report. *Arterioscler Thromb Vasc Biol.* 2017;37:49–52.

[31] Cruz-Gonzalez I, Pabón P, Rodríguez-Barbero A, Martín-Moreiras J, Pericacho M, Sánchez PL, Ramirez V, Sánchez-Ledesma M, Martín-Herrero F, Jiménez-Candil J, Maree AO, Sánchez-Rodríguez A, Martín-Luengo C, López-Novoa JM. Identification of serum endoglin as a novel prognostic marker after acute myocardial infarction. *J Cell Mol Med.* 2008;12:955–61.

[32] Haarmann A, Vollmuth C, Kollikowski AM, Heuschmann PU, Pham M, Stoll G, Neugebauer H, Schuhmann MK. Vasoactive soluble endoglin: a novel biomarker indicative of reperfusion after cerebral large-vessel occlusion. *Cells.* 2023;12:288.

[33] Vitverova B, Blazickova K, Najmanova I, Vicen M, Hyšpler R, Dolezelova E, Nemeckova I, Tebbens JD, Bernabeu C, Pericacho M, Nachtigal P. Soluble endoglin and hypercholesterolemia aggravate endothelial and vessel wall dysfunction in mouse aorta. *Atherosclerosis.* 2018;271:15–25.

[34] Gallardo-Vara E, Tual-Chalot S, Botella LM, Arthur HM, Bernabeu C. Soluble endoglin regulates expression of angiogenesis-related proteins and induction of arteriovenous malformations in a mouse model of hereditary hemorrhagic telangiectasia. *Dis Model Mech.* 2018;11:dmm034397.

[35] Smadja DM, Chocron R, Rossi E, Poitier B, Pya Y, Bekbossynova M, Peronino C, Rancic J, Roussel JC, Kindo M, Gendron N, Migliozzi L, Capel A, Perles JC, Gaussem P, Ivak P, Jansen P, Girard C, Carpentier A, Latremouille C, et al. Autoregulation of pulsatile bioprosthetic total artificial heart is involved in endothelial homeostasis preservation. *Thromb Haemost.* 2020;120:1313–22.

[36] Bernabeu C, Lopez-Novoa JM, Quintanilla M. The emerging role of TGF-beta superfamily coreceptors in cancer. *Biochim Biophys Acta.* 2009;1792:954–73.

[37] Li C, Guo B, Wilson PB, Stewart A, Byrne G, Bundred N, Kumar S. Plasma levels of soluble CD105 correlate with metastasis in patients with breast cancer. *Int J Cancer.* 2000;89:122–6.

[38] Vidal AC, Duong F, Howard LE, Wiggins E, Freedland SJ, Bhowmick NA, Gong J. Soluble endoglin (sCD105) as a novel biomarker for detecting aggressive prostate cancer. *Anticancer Res.* 2020;40:1459–62.

[39] Nogués A, Gallardo-Vara E, Zafra MP, Mate P, Marijuan JL, Alonso A, Botella LM, Prieto MI. Endoglin (CD105) and VEGF as potential angiogenic and dissemination markers for colorectal cancer. *World J Surg Oncol.* 2020;18:99.

[40] Litwiniuk M, Niemczyk K, Niderla-Bielińska J, Łukawska-Popieluch I, Grzela T. Soluble endoglin (CD105) serum level as a potential

marker in the management of head and neck paragangliomas. *Ann Otol Rhinol Laryngol.* 2017;126:717–21.

[41] Takahashi N, Kawanishi-Tabata R, Haba A, Tabata M, Haruta Y, Tsai H, Seon BK. Association of serum endoglin with metastasis in patients with colorectal, breast, and other solid tumors, and suppressive effect of chemotherapy on the serum endoglin. *Clin Cancer Res.* 2001;7:524–32.

[42] Rossi E, Sanz-Rodriguez F, Eleno N, Düwell A, Blanco FJ, Langa C, Botella LM, Cabañas C, Lopez-Novoa JM, Bernabeu C. Endothelial endoglin is involved in inflammation: role in leukocyte adhesion and transmigration. *Blood.* 2013;121:403–15.

[43] Rossi E, Smadja DM, Boscolo E, Langa C, Arevalo MA, Pericacho M, Gamella-Pozuelo L, Kauskot A, Botella LM, Gaussem P, Bischoff J, Lopez-Novoa JM, Bernabeu C. Endoglin regulates mural cell adhesion in the circulatory system. *Cell Mol Life Sci.* 2016;73:1715–39.

[44] Ruiz-Llorente L, Vega MC, Fernández FJ, Langa C, Morrell NW, Upton PD, Bernabeu C. Generation of a soluble form of human endoglin fused to green fluorescent protein. *Int J Mol Sci.* 2021;22: 11282.

[45] Decouture B, Dreano E, Belleville-Rolland T, Kuci O, Dizier B, Bazaa A, Coqueran B, Lompre AM, Denis CV, Hulot JS, Bachelot-Loza C, Gaussem P. Impaired platelet activation and cAMP homeostasis in MRP4-deficient mice. *Blood.* 2015;126:1823–30.

[46] Paszkowiak JJ, Dardik A. Arterial wall shear stress: observations from the bench to the bedside. *Vasc Endovasc Surg.* 2003;37:47–57.

[47] Dumas M, Nadal-Wollbold F, Gaussem P, Perez M, Mirault T, Létienne R, Bourbon T, Grelac F, Le Grand B, Bachelot-Loza C. Antiplatelet and antithrombotic effect of F 16618, a new thrombin proteinase-activated receptor-1 (PAR1) antagonist. *Br J Pharmacol.* 2012;165:1827–35.

[48] Martin AC, Zlotnik D, Bonete GP, Baron E, Decouture B, Belleville-Rolland T, Le Bonniec B, Poirault-Chassac S, Alessi MC, Gaussem P, Godier A, Bachelot-Loza C. Epinephrine restores platelet functions inhibited by ticagrelor: a mechanistic approach. *Eur J Pharmacol.* 2020;866:172798.

[49] Egot M, Lasne D, Poirault-Chassac S, Mirault T, Pidard D, Dreano E, Elie C, Gandrille S, Marchelli A, Baruch D, Rendu J, Fauré J, Flaujac C, Gratacap MP, Sié P, Gaussem P, Salomon R, Baujat G, Bachelot-Loza C. Role of oculocerebrorenal syndrome of Lowe (OCRL) protein in megakaryocyte maturation, platelet production and functions: a study in patients with Lowe syndrome. *Br J Haematol.* 2021;192:909–21.

[50] Drescher DG, Selvakumar D, Drescher MJ. Analysis of protein interactions by surface plasmon resonance. *Adv Protein Chem Struct Biol.* 2018;110:1–30.

[51] Saito T, Bokhove M, Croci R, Zamora-Caballero S, Han L, Letarte M, de Sanctis D, Jovine L. Structural basis of the human endoglin-BMP9 interaction: insights into BMP signaling and HHT1. *Cell Rep.* 2017;19:1917–28.

[52] Llorca O, Trujillo A, Blanco FJ, Bernabeu C. Structural model of human endoglin, a transmembrane receptor responsible for hereditary hemorrhagic telangiectasia. *J Mol Biol.* 2007;365:694–705.

[53] Frezza E, Martin J, Lavery R. A molecular dynamics study of adenylyl cyclase: the impact of ATP and G-protein binding. *PloS One.* 2018;13: e0196207.

[54] Zhu J, Luo BH, Xiao T, Zhang C, Nishida N, Springer TA. Structure of a complete integrin ectodomain in a physiologic resting state and activation and deactivation by applied forces. *Mol Cell.* 2008;32: 849–61.

[55] Takagi J, Petre BM, Walz T, Springer TA. Global conformational rearrangements in integrin extracellular domains in outside-in and inside-out signaling. *Cell.* 2002;110:599, 11.

[56] Springer TA, Zhu J, Xiao T. Structural basis for distinctive recognition of fibrinogen γC peptide by the platelet integrin αIIbβ3. *J Cell Biol.* 2008;182:791–800.

[57] Veesler D, Cupelli K, Burger M, Gräber P, Stehle T, Johnson JE. Single-particle EM reveals plasticity of interactions between the adenovirus penton base and integrin αVβ3. *Proc Natl Acad Sci USA.* 2014;111:8815–9.

[58] Pettersen EF, Goddard TD, Huang CC, Couch GS, Greenblatt DM, Meng EC, Ferrin TE. UCSF Chimera–a visualization system for exploratory research and analysis. *J Comput Chem.* 2004;25:1605–12.

[59] Suhre K, Sanejouand YH. ElNémo: a normal mode web server for protein movement analysis and the generation of templates for molecular replacement. *Nucleic Acids Res.* 2004;32:W610–4.

[60] Takagi J, Springer TA. Integrin activation and structural rearrangement. *Immunol Rev.* 2002;186:141–63.

[61] Estevez B, Shen B, Du X. Targeting integrin and integrin signaling in treating thrombosis. *Arterioscler Thromb Vasc Biol.* 2015;35:24–9.

[62] Igreja Sá IC, Tripska K, Hroch M, Hyspler R, Ticha A, Lastuvkova H, Schreiberova J, Dolezelova E, Eissazadeh S, Vitverova B, Najmanova I, Vasinova M, Pericacho M, Micuda S, Nachtigal P. Soluble endoglin as a potential biomarker of nonalcoholic steatohepatitis (NASH) development, participating in aggravation of NASH-related changes in mouse liver. *Int J Mol Sci.* 2020;21:9021.

[63] Mohammed BM, Monroe DM, Gailani D. Mouse models of hemostasis. *Platelets.* 2020;31:417–22.

[64] Li W, Nieman M, Sen Gupta A. Ferric chloride-induced murine thrombosis models. *J Vis Exp.* 2016;115:54479.

[65] Lordkipanidzé M, Lowe GC, Kirkby NS, Chan MV, Lundberg MH, Morgan NV, Bem D, Nisar SP, Leo VC, Jones ML, Mundell SJ, Daly ME, Mumford AD, Warner TD, Watson SP, UK Genotyping and Phenotyping of Platelets Study Group. Characterization of multiple platelet activation pathways in patients with bleeding as a high-throughput screening option: use of 96-well Optimul assay. *Blood.* 2014;123:e11–23.

[66] Huang J, Li X, Shi X, Zhu M, Wang J, Huang S, Huang X, Wang H, Li L, Deng H, Zhou Y, Mao J, Long Z, Ma Z, Ye W, Pan J, Xi X, Jin J. Platelet integrin αIIbβ3: signal transduction, regulation, and its therapeutic targeting. *J Hematol Oncol.* 2019;12:26.

[67] Bennett JS, Berger BW, Billings PC. The structure and function of platelet integrins. *J Thromb Haemost.* 2009;7:200–5.

[68] Holmbäck K, Danton MJS, Suh TT, Daugherty CC, Degen JL. Impaired platelet aggregation and sustained bleeding in mice lacking the fibrinogen motif bound by integrin α(Iib)β3. *EMBO J.* 1996;15: 5760–71.

[69] Hantgan RR, Stahle MC, Lord ST. Dynamic regulation of fibrinogen: integrin αIIbβ3 binding. *Biochemistry.* 2010;49:9217–25.

[70] Swieringa F, Spronk HMH, Heemskerk JWM, van der Meijden PEJ. Integrating platelet and coagulation activation in fibrin clot formation. *Res Pract Thromb Haemost.* 2018;2:450–60.

[71] Salsmann A, Schaffner-Reckinger E, Kabile F, Plançon S, Kieffer N. A new functional role of the fibrinogen RGD motif as the molecular switch that selectively triggers integrin αIIbβ3-dependent RhoA activation during cell spreading. *J Biol Chem.* 2005;280:33610–9.

[72] Bledzka K, Smyth SS, Plow EF. Integrin αIIbβ3: from discovery to efficacious therapeutic target. *Circ Res.* 2013;112:1189–200.

[73] Broos K, Feys HB, De Meyer SF, Vanhoorelbeke K, Deckmyn H. Platelets at work in primary hemostasis. *Blood Rev.* 2011;25:155–67.

SUPPLEMENTARY MATERIAL